Experimental reconstruction of nonlocal response of thermal nonlinear optical media

Alexander Minovich,[1,*] Dragomir N. Neshev,[1] Alexander Dreischuh,[1,2] Wieslaw Krolikowski,[1] and Yuri S. Kivshar[1]

[1]*Nonlinear Physics Centre and Laser Physics Centre, Research School of Physical Sciences and Engineering, Australian National University, Canberra ACT 0200, Australia*

[2]*Permanent address: Department of Quantum Electronics, Faculty of Physics, Sofia University, Bulgaria*

**Corresponding author: min124@rsphysse.anu.edu.au*

Received December 15, 2006; revised March 11, 2007; accepted April 1, 2007; posted April 11, 2007 (Doc. ID 78152); published June 5, 2007

We study experimentally and theoretically the nonlocal response of a medium with thermal nonlinearity and show that despite its inherently infinite range it can be accurately characterized by a well-defined nonlocal response function. We retrieve the shape of this function and analyze its transformation with the change of boundaries.

OCIS codes: 190.4420, 190.4870.

Optical nonlinearity is an important property of a material that characterizes its response to an external electromagnetic field. It is usually accepted that the material response at a certain point depends only on the value of the field at that point. However, the response of many materials is spatially *nonlocal*. In a nonlocal medium the nonlinear response induced at a certain point is carried away to the surrounding regions. The size of this extended region determines the range of nonlocality. In materials where the nonlinearity appears as a result of, e.g., diffusion processes, the nonlocal region expands to microscopic or even macroscopic scales.

The physical processes leading to a long-range nonlocal nonlinear response are rather diverse, including plasma heating and ionization [1], atomic diffusion [2], and drift and/or diffusion of photoexcited carriers in photorefractive media [3,4]. Similarly, the heat conduction in materials with thermal nonlinearity [5,6] results in a spatially nonlocal change of the optical refractive index often termed a "response with an infinite range of nonlocality" [7]. The physics of these nonlocal mechanisms is very different; however, the description of the nonlinear response can be unified, provided that the nonlinear change of the refractive index, $\Delta n(x,y)$, is expressed by a nonlocal response function $R(x,y)$ determining the degree of nonlocality [8,9]:

$$\Delta n(x,y) = \int\int \gamma R(x-x',y-y')I(x',y')\mathrm{d}x'\mathrm{d}y', \quad (1)$$

where $I(x,y)$ is the light intensity at the point (x,y) and γ is a normalization coefficient, such that $\int R(x,y)\mathrm{d}x\mathrm{d}y=1$. Obviously, in this approach the shape and spatial extent of the nonlocal response function are the only characteristics that determine the light propagation in such materials. In this Letter, we study experimentally and theoretically the characteristics of the nonlocal response of a thermal nonlinear liquid as a medium with an infinite extent of nonlocality. We demonstrate that, despite being inherently dependent on boundaries, the response of finite-size thermal medium can be accurately described by the generic spatially invariant nonlocal relation Eq. (1) with a well-defined, localized nonlocal response function dependent only on sample geometry.

To determine experimentally the characteristics of the nonlocal response function we use a pump–probe technique to induce a refractive index modulation in a weakly absorbing liquid. The intensity-dependent refractive index change of such a medium results from heating of the liquid by the absorbed laser light, volume expansion, and subsequent index change via the thermo-optic effect. To induce an index change, the wavelength of the pump light has to be partially absorbed by the sample. On the other hand, the sample should not be affected by the probe beam. To achieve such conditions, we use a pump laser at 532 nm and probe at 633 nm (see Fig. 1), where the intensity of the probe beam is several orders of magnitude lower than the pump intensity. Both laser beams pass through a 2 mm thick glass cell filled

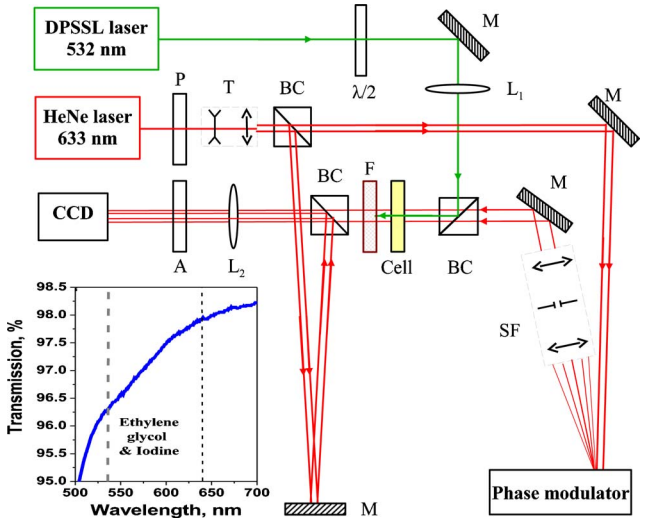

Fig. 1. (Color online) Experimental setup: F, filter; SF, spatial filter; M, mirrors; L, lenses; BC, beam-splitter cube; P, polarizer; T, telescope; λ/2, half-wave plate; A, attenuator. Inset, ethylene glycol transmission spectrum.

with liquid (ethylene glycol or ethanol) dyed with iodine. The iodine allows for higher absorption of the green pump beam than for the red probe (Fig. 1, inset).

For reconstruction of the induced refractive index distribution the cell is placed in the object arm of an adaptive interferometer [10]. It contains a programmable phase modulator as a controllable-phase mirror in a diffraction-grating regime. The modulator introduces a desired phase shift in the first diffraction order, which is selected by a spatial filter. The pump beam is combined with the probe by a pair of polarizing beam-splitter cubes. The cell is subsequently imaged onto a high-resolution CCD camera.

This interferometric technique allows one to quantitatively determine the spatial distribution of the induced refractive index change, $\Delta n(x,y)$, providing that the probe beam does not change its shape inside the cell. This condition is met in the thin cell. The subsequent phase reconstruction procedure is a particular realization of the four-frame interferometric technique [11]. In our experiment a set of four interferograms $I_j(x,y)$ $(j=1\ldots4)$ is recorded (Fig. 2, right inset) for phase shifts of $(j-1)\pi/2$ between the object and the reference beams. The phase profile in the object arm of the interferometer can then be reconstructed according to the relation $\varphi(x,y)=\tan^{-1}[(I_4-I_2)/(I_1-I_3)]$. The experiments were performed at different beam positions inside the sample away from the transverse boundaries.

The measured maximum change of the refractive index versus the absorbed laser power, shown in Fig. 2(a), is a linear dependence and agrees with earlier theoretical predictions [6]. The retrieved two-dimensional (2D) nonlinear refractive index $\Delta n(x,y)$ is shown in Figs. 2(b) and 2(c) as both 2D pseudocolor and 3D plots for ethylene glycol and ethanol, respectively. For comparison, in Fig. 2(a), left inset, we show the intensity profile of the pump laser $I_0(x,y)$, which is clearly much narrower than the induced response. In the case of ethanol, the induced refractive index is strongly asymmetric, indicating the presence of convection in the sample [6]. The convection effectively carries upward the absorbed heat, reducing the size of the nonlocal response in the horizontal direction.

Having the index distribution and the pump-beam intensity profile, we determine the nonlocal response function $R(x,y)$. This is essentially an inverse problem [12], which is solved iteratively by Fourier deconvolution as $R(x,y)=\mathcal{F}^{-1}\{\mathcal{F}[\Delta n(x,y)]/\mathcal{F}[I(x,y)]\}$. The dependence of the full width at half-maximum (FWHM) of the response function in the horizontal x direction for both liquids is shown in Fig. 3(a). In the case of ethylene glycol the width of the response function is independent of power, which is expected, as the response function should not depend on the width or intensity of the input beam. On the other hand, the width of the response function is reduced with power in the case of ethanol. This is a consequence of the convection process, being power dependent. At low powers where no convection is present the response function has the same profile for both liquids. To understand why these two significantly different materials have the same response function (in the absence of convection) we consider the heat equation in a medium with thermal conductivity k and linear absorption α,

$$k\nabla^2 T(x,y,z) = -\alpha I(x,y), \tag{2}$$

where $T(x,y,z)$ is the temperature distribution in the sample and ∇^2 is the Laplacian. The temperature distribution inside the sample determines the induced refractive index change by $\Delta n(x,y,z)=(dn/dT)\Delta T$, where dn/dT is the thermo-optic coefficient of the material. For boundaries with constant temperature the solution of heat equation (2) can be written as $T(x,y,z)=\alpha/k\int\int\int I(x',y')G(x,x',y,y',z,z')dx'dy'dz'$,

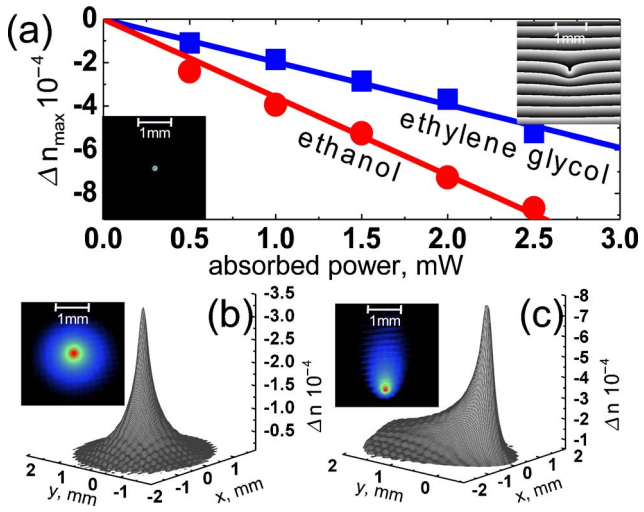

Fig. 2. (Color online) (a) Dependence of peak refractive index change on absorbed power. Right inset, measured interference pattern (ethylene glycol, 2 mW); left inset, laser beam profile. (b), (c) Reconstructed refractive index change profiles in ethylene glycol and ethanol at 2 mW.

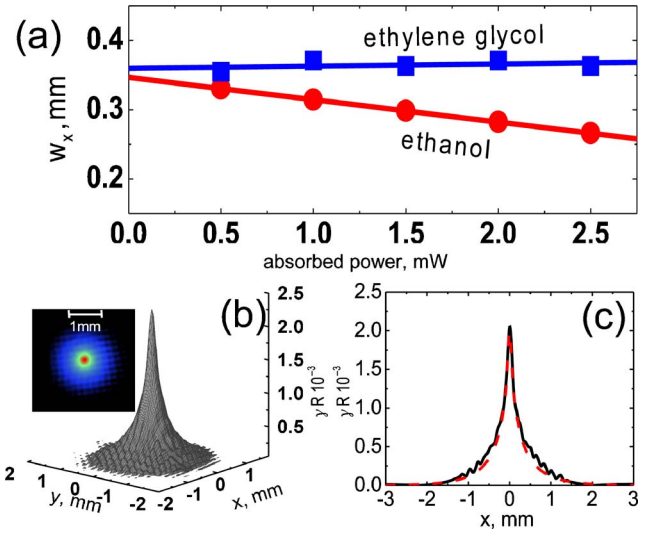

Fig. 3. (Color online) (a) Dependence of the response function FWHM (w_x) on absorbed power. (b), (c) Reconstructed response function profile (b) and comparison of the measured (solid line) and calculated (dashed) response function profile (c) for ethylene glycol.

where $G(x,x',y,y',z,z')$ is a Green function that depends on the geometry and boundary conditions only. Now one can remove the z dependence from the refractive index change $\Delta n(x,y,z)$ by integrating it along the sample length L. Then we obtain $\Delta n(x,y) = (dn/dT)/L\int_0^L T(x,y,z)dz$. Therefore the response function calculated by inverting relation Eq. (1) indeed depends only on the geometry of the sample and the boundary conditions, but not on the properties of the medium, confirming our experimental observations. In Fig. 3(b) and 3(c) we show the spatial profile of the retrieved nonlocal response function $R(x,y)$. The agreement with the profile calculated by using the heat equation (2) is excellent, as shown in Fig. 3(c). The above representation also applies for the case of an asymmetric boundary condition leading to an asymmetric response function $R(x,y)$.

The dependence of thermal nonlinearity on boundaries has serious consequences for the index measurements. Typically, in the context of beam propagation in a thick thermal sample only the transverse geometry is considered. In a thick sample the slow variation of the beam intensity along the propagation direction does not lead to any appreciable temperature gradient or heat flow in this direction. As a result, the nonlocal response is a function of the transverse coordinates only. The situation becomes more complex when a thin sample is used (as in our experiments). In this case the front and back facets of the cell induce longitudinal heat flow, affecting the final temperature and refractive index distributions, which become a function of three spatial coordinates. To assess the impact of this effect on the nonlocal response function we solved numerically Eq. (2) assuming a Gaussian pump beam as a heat source. In the simulations the transverse dimensions of the sample were kept constant while the thickness was varied. Figure 4 shows the calculated width of the response function (top) and corresponding maximum refractive index change (bottom) versus the sample thickness. It is clear that for thin samples the heat flow toward the back and front boundaries strongly affects the measured index distribution, thus decreasing the range of nonlocality in transverse direction.

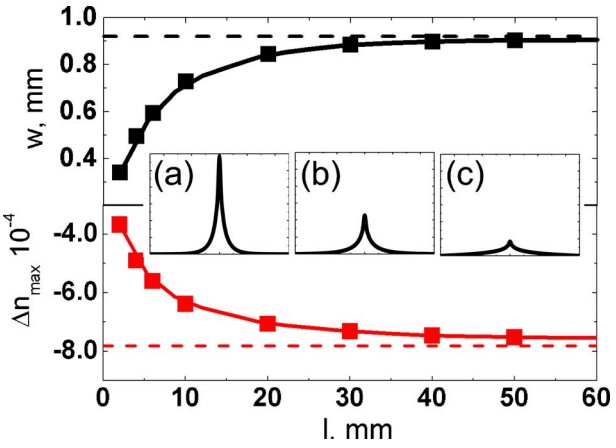

Fig. 4. (Color online) Calculated width of the response function (top) and corresponding maximum of the refractive index change (bottom) as a function of the cell thickness. (a)–(c) Radical profiles of the response function for thicknesses of 2, 4, and 50 mm, respectively.

On the other hand, when the thickness of the sample increases, the effect of longitudinal heat flow becomes less pronounced until the response is completely determined by the transverse boundaries. However, in all cases the nonlocality can still be well described by the generic convolution model, Eq. (1). In fact this approximation is more accurate for a thin sample when the influence of transverse boundaries on the heat flow is weaker. The insets in Fig. 4 depict profiles of the response function calculated for thicknesses of 2, 4, and 50 mm. The increase of the extent of nonlocality and change of its shape with sample thickness is clearly visible.

In conclusion, we have demonstrated that nonlocal nonlinearity of a thermal medium can be described accurately by a finite-extent nonlocal response function even though the thermal effect is of an infinite range. The response function is independent of the material parameters and is determined by the geometry of the sample. Therefore control of the remote boundaries provides an efficient tool for affecting the propagation of beams in thermal nonlinear media [13].

The work was supported by the Australian Research Council and the National Science Fund (Bulgaria, F-1303).

References

1. A. Litvak, V. Mironov, G. Fraiman, and A. Yunakovskii, Sov. J. Plasma Phys. **1**, 31 (1975).
2. D. Suter and T. Blasberg, Phys. Rev. A **48**, 4583 (1993).
3. S. Gatz and J. Herrmann, Opt. Lett. **23**, 1176 (1998).
4. B. Crosignani, A. Degasperis, E. DelRe, P. Di Porto, and A. J. Agranat, Phys. Rev. Lett. **82**, 1664 (1999).
5. J. P. Gordon, R. C. C. Leite, R. S. Moore, S. P. S. Porto, and J. R. Whinnery, J. Appl. Phys. **36**, 3 (1965).
6. S. A. Akhmanov, D. P. Krindach, A. V. Migulin, A. P. Sukhorukov, and R. V. Khokhlov, IEEE J. Quantum Electron. **QE–4**, 568 (1968).
7. C. Rotschild, O. Cohen, O. Manela, M. Segev, and T. Carmon, Phys. Rev. Lett. **95**, 213904 (2005).
8. J. Wyller, W. Krolikowski, O. Bang, and J. J. Rasmussen, Phys. Rev. E **66**, 066615 (2002).
9. W. Krolikowski, O. Bang, N. I. Nikolov, D. Neshev, J. Wyller, J. J. Rasmussen, and D. Edmundson, J. Opt. B **6**, S288 (2004).
10. J. Leach, E. Yao, and M. J. Padgett, New J. Phys. **6**, 71 (2004).
11. C. Creath, *Holographic Interferometry* (Springer, 1994).
12. L. L. Gurdev, T. N. Dreischuh, and D. V. Stoyanov, J. Opt. Soc. Am. A **10**, 2296 (1993).
13. C. Rotschild, B. Alfassi, O. Cohen, and M. Segev, Nat. Phys. **2**, 769 (2006).